

Power Amplifier Design Fundamentals: More Notes from the Pages of History

By Andrei Grebennikov
Bell Labs Ireland

This is the conclusion of an article that examines the historical foundations of the principles that built our knowledge of power amplifier operation

Amplifier Stability

In early radio-frequency vacuum-tube transmitters, it was observed that the tubes and associated circuits may have damped or undamped oscillations depending upon the circuit losses, the feedback coupling, the grid and anode potentials, and the reactance or tuning of the parasitic circuits [28]. Various parasitic oscillator circuits such as the tuned-grid-tuned-anode circuit with capacitive feedback, Hartley, Colpitts, or Meissner oscillators can be realized at high frequencies which potentially can be eliminated by adding a small resistor close to the grid or anode connections of the tubes for damping the circuits. Inductively coupled rather than capacitively coupled input and output circuits should be used wherever possible.

According to the immittance approach to the stability analysis of the active nonreciprocal two-port network, it is necessary and sufficient for its unconditional stability if the following system of equations can be satisfied for the given active device:

$$\operatorname{Re}[W_s(\omega) + W_{in}(\omega)] > 0 \quad (22)$$

$$\operatorname{Im}[W_s(\omega) + W_{in}(\omega)] = 0 \quad (23)$$

or,

$$\operatorname{Re}[W_L(\omega) + W_{out}(\omega)] > 0 \quad (24)$$

$$\operatorname{Im}[W_L(\omega) + W_{out}(\omega)] = 0 \quad (25)$$

where $\operatorname{Re}W_s$ and $\operatorname{Re}W_L$ are considered to be greater than zero [29, 30]. The active two-port

network can be treated as unstable or potentially unstable in the case of the opposite signs in Eqs. (22) and (24).

Analysis of Eq. (22) or Eq. (24) on extremum results in a special relationship between the device immittance parameters called the device stability factor

$$K = \frac{2 \operatorname{Re} W_{11} \operatorname{Re} W_{22} - \operatorname{Re}(W_{12} W_{21})}{|W_{12} W_{21}|} \quad (26)$$

which shows a stability margin indicating how far from zero value are the real parts in Eqs. (22) and (24) being positive [30]. In this case, an active device is unconditionally stable if $K \geq 1$ and potentially unstable if $K < 1$.

When the active device stability factor $K > 1$, the operating power gain G_p has to be maximized. By analyzing Eq. (19) on extremum, it is possible to find optimum values $\operatorname{Re}W_L^o$ and $\operatorname{Im}W_L^o$ when the operating power gain G_p is maximal [31, 32]. As a result,

$$G_{P_{\max}} = \frac{|W_{21}|}{|W_{12}|} / (K + \sqrt{K^2 - 1}) \quad (27)$$

The power amplifier with an unconditionally stable active device provides a maximum power gain operation only if the input and output of the active device are conjugate-matched with the source and load impedances, respectively. For the lossless input matching circuit when the power available at the source is equal to the power delivered to the input port of the active device, that is $P_S = P_{in}$, the maximum operating power gain $G_{P_{\max}}$ is equal to the maximum transducer power gain $G_{T_{\max}}$.

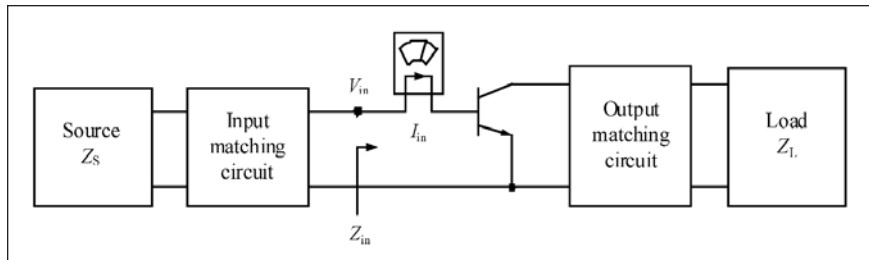


Figure 5 · Single-stage power amplifier with measured device input impedance.

Domains of the device potential instability include the operating frequency ranges where the active device stability factor is equal to $K < 1$. Within the bandwidth of such a frequency domain, parasitic oscillations can occur, defined by internal positive feedback and operating conditions of the active device. The instabilities may not be self-sustaining, being induced by the RF drive power but remaining on its removal. One of the most serious cases of power amplifier instability can occur when there is a variation of the load impedance. Under these conditions, a transistor may be destroyed almost instantaneously. But even it is not destroyed, the instability can result in a tremendously increased level of the spurious emissions in the output spectrum of the power amplifier. Generally, the following classification for instabilities can be made [33, 34]:

1. *Linear*—low-frequency oscillations produced by thermal feedback effects; oscillations due to internal feedback; negative resistance or conductance induced instabilities due to transit-time effects, or avalanche multiplication; and oscillations due to external feedback as a result of insufficient decoupling of the DC supply.
2. *Nonlinear*—parametric generation of harmonics or subharmonics when the large-signal drive acts like pumping a varactor-type collector-base capacitance.

It should be noted that expressions in Eqs. (22) to (27) are given through the device immittance Z - or Y -parameters that allows the power gain and stability to be calculated using the parameters of the device equivalent circuit and to physically understand the corresponding effect of each circuit parameter, but not through scattering S -parameters, which are very convenient during the measurement procedure required for device modeling. Moreover, using modern simulation tools, it is even no need to draw stability circles on a Smith chart or analyze stability factor across the wide frequency range since K -factor is just a derivation from the basic stability conditions and usually is a function of linear parameters which can only reveal linear instabilities. Besides, it is difficult

to predict unconditional stability for a multistage power amplifier because parasitic oscillations can be caused by the interstage circuits. In this case, the easiest and most effective way to provide stable operation of the multistage power amplifier (or single-stage power amplifier) is to simulate the real part of the device input impedance $Z_{in} = V_{in} / I_{in}$ at the input terminal of each transistor as a ratio between the input voltage and current by placing a voltage node and a current

meter, as shown in Fig. 5. If $\text{Re}Z_{in} < 0$, then either a small series resistor must be added to the device base terminal as a part of the input matching circuit or a load network configuration properly chosen to provide the resulting positive value of $\text{Re}Z_{in}$. In this case, not only linear instabilities with small-signal soft startup oscillation conditions but also nonlinear instabilities with large-signal hard startup oscillation conditions or parametric oscillations can be identified around operating region.

Effect of Higher-Order Harmonics

In some practical cases, it is somewhat difficult to implement the parallel-tuned output circuit required for conventional Class C operation in power amplifiers employing either field-effect or bipolar transistors, as the inductance can be very small with sufficient effect of the device package parasitics. In addition, the dependence of the collector capacitance on the output voltage in the power amplifier represents a nonlinear varactor-junction function which makes it difficult to maintain a sinusoidal collector voltage waveform. A nonlinear capacitance in parallel with an inductance does not act as a simple resonant circuit, and produces a voltage waveform containing harmonics in response to a sinusoidal current. In contrast, the series-tuned resonant circuit or low-pass LC -type output matching circuit with series inductor used in a dual-mode Class C operation can eliminate some problems relevant to a conventional Class C mode and improve power amplifier performance since it allows the presence of harmonic components in the collector voltage, while preventing harmonic currents [35].

An effect of the nonlinear collector capacitance on electrical behavior of the power amplifier can be analyzed based on the equivalent power amplifier circuit including a series resonant L_0C_0 circuit tuned to the fundamental frequency that provides open-circuit conditions for second and higher order harmonic components of the output current, and an L-type matching circuit with the series inductor L and shunt capacitor C , as shown in Figure 6(a). The matching circuit is required to match the equivalent output resistance R , corresponding to the required maximum output power at the fundamental frequency, with the stan-

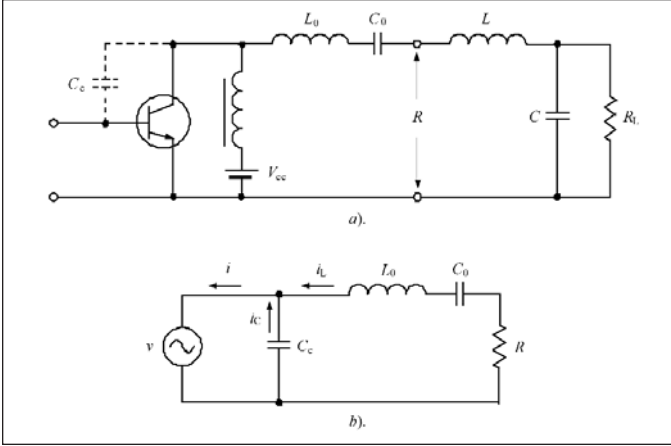


Figure 6 · Class C mixed-mode power amplifier circuit schematics.

standard load resistance R_L . Figure 6(b) shows the simplified output equivalent circuit of the bipolar power amplifier.

The total output current flowing through the device collector can be written as

$$i = I_0 + \sum_{n=1}^{\infty} I_n \cos(n\omega t + \phi_n) \quad (28)$$

where I_n and ϕ_n are the amplitude and phase of the n th harmonic component, respectively. An assumption of a high quality factor of the series resonant circuit allows only the fundamental-frequency current component to flow into the load. The current flowing through the nonlinear collector capacitance consists of the fundamental-frequency and higher harmonic components:

$$i_c = I_C \cos(\omega t + \phi_1) + \sum_{n=2}^{\infty} I_n \cos(n\omega t + \phi_n) \quad (29)$$

where I_C is the fundamental-frequency capacitor current amplitude.

The nonlinear behavior of the collector junction capacitance is described by

$$C_c = C_0 \left(\frac{\phi + V_{cc}}{\phi + v} \right)^\gamma \quad (30)$$

where C_0 is the collector capacitance at $v = V_{cc}$, V_{cc} is the supply voltage, ϕ is the contact potential, and γ is the junction sensitivity equal to 0.5 for abrupt junction. As a result, the expression for charge flowing through collector capacitance can be obtained by

$$q = \int_0^v C_c(v) dv = \int_0^v \frac{C_0 (\phi + V_{cc})^\gamma}{(\phi + v)^\gamma} dv \quad (31)$$

Solving Eq. (31) for v , substituting Eq. (29), applying Taylor expansion, and then equating the fundamental-voltage collector voltage components results in

$$\begin{aligned} \sigma_p = 1 + \frac{I_2 \gamma}{4\omega C_0 V_{cc}} \cos(90^\circ + \phi_2 - 2\phi_1) \\ + \frac{I_2 I_3 \gamma}{12(\omega C_0)^2 V_1 V_{cc}} \cos(90^\circ + \phi_3 - \phi_2 - \phi_1) \end{aligned} \quad (32)$$

where $\sigma_p = \xi_p / \xi$, ξ_p is the collector voltage peak factor with parametric effect, $\xi = V_1 / V_{cc}$, and V_1 is the fundamental-frequency voltage amplitude [36].

From Eq. (32) it follows that, to maximize the collector voltage peak factor and, consequently, the collector efficiency for a given value of the supply voltage V_{cc} , it is necessary to provide the following phase conditions:

$$\phi_2 = 2\phi_1 - 90^\circ \quad (33)$$

$$\phi_3 = 3\phi_1 - 180^\circ \quad (34)$$

Then, for $\gamma = 0.5$,

$$\sigma_p = 1 + \frac{I_2}{8\omega C_0 V_{cc}} + \frac{I_2 I_3}{24(\omega C_0)^2 V_1 V_{cc}} \quad (35)$$

Equation (35) shows the theoretical possibility to increase the collector voltage peak factor by 1.1 to 1.2 times, thus achieving collector efficiency of 85 to 90%. Physically, the improved efficiency can be explained by the parametric transformation of powers corresponding to the second and higher-order harmonic components into the fundamental-frequency output power because of the nonlinearity of the collector capacitance. However, this becomes effective only in the case of the load network with a series resonant circuit, since it ideally provides infinite impedance at the second and higher-order harmonic components, unlike the load network with a parallel resonant circuit having ideally zero impedance at these harmonics.

Realizing biharmonic or polyharmonic operation modes of the vacuum-tube power amplifiers, using resonant circuits tuned to the odd or even harmonics of the fundamental frequency in the load network, is very effective for increasing their operating efficiency [37]. Ideally, this implies the in-phase or out-of-phase harmonic conditions for symmetrical flattened voltage or current waveforms can be formed. However, as it turned out, this is not the only way to improve the power amplifier efficiency with a resonant circuit in the load network. Figure 7 shows the circuit schematic of the vacuum-tube power amplifier with a parallel-tuned resonant circuit inserted between the anode and the output matching circuit, which

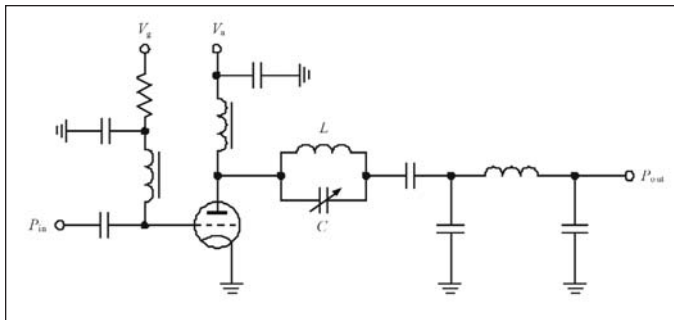


Figure 7 · Class C power amplifier with detuned resonant circuit.

has a resonant frequency equal to about 1.5 times the carrier frequency of the signal to be amplified [38]. In other words, if the carrier signal is transmitting at a fundamental frequency f_0 , the parallel resonant circuit will have a resonant frequency of about $1.5f_0$ followed by a filter or output matching circuit to suppress the harmonics of the fundamental frequency and to maximize the output power at the fundamental frequency delivered to the standard load. As a result, an efficiency of 89% was achieved for a 3.2 MHz vacuum-tube high-power amplifier.

Although it was assumed that such a parallel resonant circuit introduces considerable impedance to its own second harmonic—which is the third harmonic $3f_0$ of the carrier frequency—and can result in a flattened anode voltage waveform, another interesting and nontrivial conclusion can be derived from this circuit topology. In this case, provided the output p-type matching circuit has purely resistive impedance at the fundamental frequency and capacitive reactances at the harmonic components, the anode of the device sees inductive impedance at the fundamental frequency and capacitive reactances at the second and higher-order harmonic components. This means that the voltage and current waveforms are not symmetrical anymore, thus representing an alternative mechanism of the efficiency improvement. Such an effect of increasing efficiency when the output resonant circuit of the vacuum-tube or transistor Class C power amplifier is detuned relative to the carrier frequency (tuned slightly above resonance) was described a few years before [39, 40]. The anode efficiencies of about 92-93% were achieved for the phase angles of the load network being in between $+30^\circ$ and $+40^\circ$ and resulting in the inductive impedance at the fundamental frequency and capacitive reactances at the harmonic components seen by the anode of the active device [39].

A decade later, these experimental results were confirmed by the theoretical verification with optimum load-network parameters, resulting in the well-known idealized collector voltage and current waveforms satisfying the Class E requirements specified for infinite number of

harmonics. This means that, similar to Class F mode which is referred to any harmonic approximations (including infinite number of harmonics as an idealized case when the active device represents an ideal switch), Class E mode corresponds to any harmonic approximations as well and can only be considered as a switching mode when the active device represents an ideal switch with control of the infinite number of harmonics and rectangular drive to fully transform the DC power into the fundamental-frequency power delivered to the load. The idealized switch assumption allows the Class E load network parameters to be exactly analytically derived in time domain. However, its basic difference from Class F mode lies in asymmetric collector voltage and current waveforms due to different load-network impedance conditions: inductive impedance at fundamental frequency and capacitive reactances for the second and higher-order harmonics (vice versa for inverse Class E). In the case of a small number of harmonics used for control, the active device can be characterized by the multiharmonic current source and Class E mode can simply be considered as a detuned case of Class C mode with a sinusoidal drive. As a result, all possible classes of amplification having their own physical and design principles and based on any number of harmonics, namely applicable to Class C (with particular cases of classes A, AB, and B), Class E, and Class F, can be closely tied with each other and the transition between them can be easily provided [41].

The first part of this article was published in the May 2010 issue. It is available for download in the Archives section of www.highfrequencyelectronics.com

Author Information

Andrei Grebennikov received the MSc degree in electronics from Moscow Institute of Physics and Technology, and the Ph.D. degree in radio engineering from Moscow Technical University of Communications and Informatics. He can be reached by e-mail at: grandrei@ieee.org

References

1. J. H. Morecroft & H. T. Friis, "The Vacuum Tubes as a Generator of Alternating-Current Power," *Trans. AIEE*, 38, pp. 1415-1444, Oct. 1919.
2. D. C. Prince, "Vacuum Tubes as Power Oscillators, Part I," *Proc. IRE*, 11, pp. 275-313, June 1923.
3. A. A. Oswald, "Power Amplifiers in Trans-Atlantic Radio Telephony," *Proc. IRE*, 13, pp. 313-324, June 1925.
4. L. E. Barton, "High Audio Power from Relatively Small Tubes," *Proc. IRE*, 19, pp. 1131-1149, July 1931.
5. C. E. Fay, "The Operation of Vacuum Tubes as Class B and Class C Amplifiers," *Proc. IRE*, 20, pp. 548-568, Mar. 1932.
6. P. H. Osborn, "A Study of Class B and C Amplifier Tank Circuits," *Proc. IRE*, 20, pp. 813-834, May 1932.

7. A. I. Berg, *Theory and Design of Vacuum-Tube Generators* (in Russian), Moskva: GEI, 1932.
8. F. E. Terman & J. H. Ferns, "The Calculation of Class C Amplifier and Harmonic Generator Performance of Screen-Grid and Similar Tubes," *Proc. IRE*, 22, pp. 359-373, Mar. 1934.
9. L. B. Hallman, "A Fourier Analysis of Radio-Frequency Power Amplifier Wave Forms," *Proc. IRE*, 20, pp. 1640-1659, Oct. 1932.
10. W. L. Everitt, "Optimum Operating Conditions for Class C Amplifiers," *Proc. IRE*, 22, pp. 152-176, Feb. 1934.
11. C. E. Kilgour, "Graphical Analysis of Output Tube Performance," *Proc. IRE*, 19, pp. 42-50, Jan. 1931.
12. D. C. Espley, "The Calculation of Harmonic Production in Thermionic Valves with Resistive Load," *Proc. IRE*, 21, pp. 1439-1446, Oct. 1933.
13. V. I. Kaganov, *Transistor Radio Transmitters* (in Russian), Moskva: Energiya, 1976.
14. W. L. Everitt, "Output Networks for Radio-Frequency Power Amplifiers," *Proc. IRE*, 19, pp. 725-737, May 1931.
15. H. T. Friis, "Noise Figure of Radio Receivers," *Proc. IRE*, 32, pp. 419-422, July 1944.
16. S. Roberts, "Conjugate-Image Impedances," *Proc. IRE*, 34, pp. 198-204, Apr. 1946.
17. S. J. Haefner, "Amplifier-Gain Formulas and Measurements," *Proc. IRE*, 34, pp. 500-505, July 1946.
18. L. Pritchard, "High-Frequency Power Gain of Junction Transistors," *Proc. IRE*, 43, pp. 1075-1085, Sept. 1955.
19. A. R. Stern, "Stability and Power Gain of Tuned Power Amplifiers," *Proc. IRE*, 45, pp. 335-343, Mar. 1957.
20. L. S. Houselander, H. Y. Chow, & R. Spense, "Transistor Characterization by Effective Large-Signal Two-Port Parameters," *IEEE J. Solid-State Circuits*, SC-5, pp. 77-79, Apr. 1970.
21. E. F. Belohoubek, A. Rosen, D. M. Stevenson, & A. Pressser, "Hybrid Integrated 10-Watt CW Broad-Band Power Source at S Band," *IEEE J. Solid-State Circuits*, SC-4, pp. 360-366, Dec. 1969.
22. A. Presser and E. F. Belohoubek, "1-2 GHz High Power Linear Transistor Amplifier," *RCA Rev.*, 33, pp. 737-751, Dec. 1972.
23. J. M. Cusack, S. M. Perlow, & B. S. Perlman, "Automatic Load Contour Mapping for Microwave Power Transistors," *IEEE Trans. Microwave Theory Tech.*, MTT-12, pp. 1146-1152, Dec. 1974.
24. Y. Takayama, "A New Load-Pull Characterization Method for Microwave Power Transistors," *1976 IEEE MTT-S Int. Microwave Symp. Dig.*, pp. 218-220.
25. G. P. Bava, U. Pisani, & V. Pozzolo, "Active Load Technique for Load-Pull Characterization at Microwave Frequencies," *Electronics Lett.*, 18, pp. 178-180, Feb. 1982.
26. C. Rauscher & H. A. Willing, "Simulation of Nonlinear Microwave FET Performance Using a Quasi-Static Model," *IEEE Trans. Microwave Theory Tech.*, MTT-27, pp. 834-840, Oct. 1979.
27. R. B. Stancliff & D. D. Poulin, "Harmonic Load-Pull," *1979 IEEE MTT-S Int. Microwave Symp. Dig.*, pp. 185-187.
28. G. W. Fyler, "Parasites and Instability in Radio Transmitters," *Proc. IRE*, 23, pp. 985-1012, Sept. 1935.
29. F. B. Llewellyn, "Some Fundamental Properties of Transmission Systems," *Proc. IRE*, 40, pp. 271-283, Mar. 1952.
30. D. F. Page & A. R. Boothroyd, "Instability in Two-Port Active Networks," *IRE Trans. Circuit Theory*, CT-5, pp. 133-139, June 1958.
31. J. M. Rollett, "Stability and Power Gain Invariants of Linear Two-Ports," *IRE Trans. Circuit Theory*, CT-9, pp. 29-32, Jan. 1962.
32. J. G. Linvill & L. G. Schimpf, "The Design of Tetrode Transistor Amplifiers," *Bell Sys. Tech. J.*, 35, pp. 813-840, Apr. 1956.
33. D. R. Lohrmann, "Parametric Oscillations in VHF Transistor Power Amplifiers," *Proc. IEEE*, 54, pp. 409-410, March 1966.
34. O. Muller & W. G. Figel, "Stability Problems in Transistor Power Amplifiers," *Proc. IEEE*, 55, pp. 1458-1466, Aug. 1967.
35. B. E. Rose, "Notes on Class D Transistor Amplifiers," *IEEE J. Solid-State Circuits*, SC-4, pp. 178-179, June 1969.
36. V. L. Aronov, "Using Nonlinear Properties of Collector Capacitance to Increase Efficiency of High-Frequency Power Amplifier (in Russian)," *Poluprovodnikovye Pribory i Ikh Primenenie*, 21, pp. 290-293, 1969.
37. A. Grebennikov, "High-Efficiency Power Amplifiers: Turning the Pages of Forgotten History," *High Frequency Electronics*, 7, pp. 18-26, Sept. 2008.
38. J. W. Wood, "High Efficiency Class C Amplifier," U.S. Patent 3,430,157, Feb. 1969 (filed Nov. 1966).
39. E. P. Khmel'nitskiy, *Operation of Vacuum-Tube Generator on Detuned Resonant Circuit* (in Russian), Moskva: Svyazizdat, 1962.
40. T. M. Scott, "Tuned Power Amplifiers," *IEEE Trans. Circuit Theory*, CT-11, pp. 385-389, Sept. 1964.
41. F. H. Raab, "Class-E, Class-C, and Class-F Power Amplifiers Based Upon a Finite Number Harmonics," *IEEE Trans. Microwave Theory Tech.*, MTT-49, pp. 1462-1468, Aug. 2001.